Applied Catalysis B: Environmental 166–167 (2015) 327–334

Contents lists available at ScienceDirect

Applied Catalysis B: Environmental

journal homepage: www.elsevier.com/locate/apcatb

Quantitative conversion of triglycerides to hydrocarbons over hierarchical ZSM-5 catalyst

Hao Chen [a], Qingfa Wang [a,b,*], Xiangwen Zhang [a,b], Li Wang [a,b]

[a] Key Laboratory of Green Chemical Technology of Ministry of Education, School of Chemical Engineering and Technology, Tianjin University, Tianjin 300072, China

[b] Collaborative Innovation Center of Chemical Science and Engineering (Tianjin), Tianjin University, Tianjin 300072, China

ARTICLE INFO

Article history:
Received 21 August 2014
Received in revised form 2 November 2014
Accepted 18 November 2014
Available online 25 November 2014

Keywords:
Hierarchical catalyst
NH_4^+ exchange
Acidity
Triglycerides
Aromatics

ABSTRACT

Hierarchical ZSM-5 was prepared by desilication with 0.5 M NaOH and ion-exchanged in NH_4NO_3 aqueous solution with different NH_4^+ concentrations. The quantitative selectivity for paraffins and aromatics in the conversion of triglycerides was investigated by tailoring the Lewis and Brønsted sites distribution of these hierarchical catalysts through the ion exchange process. The amount of Brønsted acidity in ZSM-5 increased with the NH_4^+ exchange degree, meanwhile the textural properties and Lewis acidity changed little. The untreated NiMo/ZSM-5 sample exhibited the small extent of cracking and high selectivity of C_{16}–C_{18} hydrocarbons (79.47%) because of low Brønsted acidity. The C_4–C_8 hydrocarbons with few aromatics became the dominant products for the samples treated by low NH_4NO_3 concentration (less than 0.01 M). As the concentration of NH_4^+ further increased, the aromatics began to be detected and became the major products due to the high Brønsted acidity density. The mechanism of aromatic formation was presumed. The olefins obtained by cracking and dehydrogenation were converted into cycloalkanes by Diels–Alder cyclization on Lewis acid sites. And then the cycloalkanes were transferred to Brønsted acid sites to form the aromatics by dehydrogenation–aromatization. These results showed that the desirable products could be obtained by modifying the acid distribution of the support.

1. Introduction

The development of renewable and clean fuels has become imperative due to the diminishing petroleum resources along with the continuous increasing demand for energy, and the escalating global environmental problems [1,2]. Therefore, the catalytic processing of biomass such as cellulose, lignin, and triglycerides into alternative and green biofuels attracted considerable attention because of their alternative sources, renewability and reuse of CO_2 [3,4]. Triglycerides, the major components of vegetable oils and animals fats, can be used to make liquid fuels [5]. Currently, there are two important ways to convert triglycerides into useful fuels: transesterification and hydroconversion. Transesterification of triglycerides with methanol to produce fatty acid methyl ester (FAME) is commonly used to produce biodiesel which is known as the first generation biofuel [6,7]. However, the low energy content, poor storage stability and cold-flow properties limit its development due to the high oxygen content in fuels [8]. Recently, hydroconversion of triglycerides to *produce* hydrocarbons has been considered as an alternative way to produce high quality fuel [9]. Desirable products ranging from gasoline to diesel fraction with excellent properties have been obtained with various kinds of catalysts [10–14]. The reaction pathways have also been widely studied using different vegetable oils such as canola oil, sunflower oil, soybean oil, rapeseed oil, and palm oil as well as the fatty acid fraction and/or the mixtures [15]. The side reaction of aromatization is inevitable for the acidic catalysts in the hydroconversion of the vegetable oils [16–18]. The aromatic content is an important factor to oils for their high properties [16,19,20]. Moreover, the aromatics such as benzene, toluene and xylene are also the important chemicals [21]. Although the suitable aromatic content is helpful for the transport fuels, the aromatization is considered as the undesirable side reaction for the hydroconversion of vegetable oils for now [22]. Therefore, it is very important to study how to regulate and control the reactions to quantitatively convert triglycerides into gasoline, diesel-range hydrocarbons and aromatics. But up to now it is still limited. Moreover, few works focus on the aromatic formation

* Corresponding author at: Key Laboratory of Green Chemical Technology of Ministry of Education, School of Chemical Engineering and Technology, Tianjin University, Tianjin 300072, China. Tel.: +86 22 27892340; fax: +86 22 27892340.
E-mail address: qfwang@tju.edu.cn (Q. Wang).

http://dx.doi.org/10.1016/j.apcatb.2014.11.041
0926-3373/

Table 1
Physical properties and fatty acids composition of soybean oil.

Soybean oil	Values
Fatty acid composition, wt%	
Stearic acid ($C_{18:0}$)	5.0
Oleic acid ($C_{18:1}$)	24.2
Linoleic acid ($C_{18:2}$)	56.3
Palmitic acid ($C_{16:0}$)	10.7
Other acids	4.8

mechanism in deep for the hydroconversion process of vegetable oil.

During the hydrotreating process, the support of catalyst plays a significant role in the whole reaction. Nowadays, many materials like SiO_2, TiO_2, SAPO-11, HBEA and ZSM-22 have been used as the supports for the hydroconversion of vegetable oil to hydrocarbons [23–26]. Recently, considerable attention has been paid to hierarchical materials in catalysis application [27–30]. Hierarchical ZSM-5 was designed and synthesized for hydroconversion of jatropha oil to produce aviation fuel with high *i*-alkanes/*n*-alkanes ratio [11]. The introduction of hierarchical porosity into ZSM-5 enhanced accessibility and diffusion to hinder secondary cracking reaction [31]. But it increased the proportion of light olefins in the products at the expense of aromatic compounds. In addition, hierarchical ZSM-5 has also been widely used in the field of Fischer-Tropsch synthesis [28,32]. However, although the hierarchical catalysts have been investigated so much in recent years, the influence of NH_4^+ ion exchange process on the product distribution is still unclear for the hierarchical zeolites by desilication.

In this work, the hierarchical ZSM-5 was prepared by desilication and exchanged with different concentration of NH_4NO_3 solution to tune the acidity of the catalyst. The objective was to explore the role of Lewis and Brønsted sites on the products distribution during the hydroconversion of soybean oil. The formation mechanism of aromatics was also discussed.

2. Materials and methods

2.1. Materials

The ZSM-5 with Si/Al ratio of 54.0 was supplied by Shanghai Novel Chemical Technology Co., Ltd. $(NH_4)_6Mo_7O_{24}{\cdot}4H_2O$ (≥99.0 wt%, J&K) and $Ni(NO_3)_2{\cdot}6H_2O$ (≥98.0 wt%, Alfa Aesar) were used as the Mo and Ni sources, respectively. Pyridine (99.8 wt%), cyclohexane, ammonium nitrate and sodium hydroxide were used as received.

Soybean oil was purchased from Shandong Bohi Industry Co., Ltd. The physical and chemical properties of soybean oil are presented in Table 1. The fatty acid component of the soybean oil consisted of the C_{18} acid species ($C_{18:0}$, stearic acid, $C_{18:1}$, oleic acid, $C_{18:2}$, linoleic acid, 85.5 wt%) and C_{16} acid ($C_{16:0}$, 10.7 wt%).

2.2. Catalysts preparation

The hierarchical ZSM-5 samples were prepared by a simple alkali treatment method [32]. In a typical run, original ZSM-5 was added into 0.5 M NaOH aqueous solutions ($volume_{NaOH}/weight_{ZSM\text{-}5}$ = 10.0 ml/g). The mixture was heated to 70 °C and stirred at this temperature for 1 h. Then the slurry was cooled to the room temperature. The zeolite was filtrated and washed to neutral with deionized water. The product was dried at 120 °C for 12 h and exchanged with NH_4NO_3 aqueous solution (0, 0.0005, 0.01, 0.02, 0.2, and 1.0 M) at 80 °C for 1 h. Then the samples were kept overnight, dried at 120 °C for 12 h and finally calcinated at 500 °C (heating rate 5 °C/min) for 4 h. The obtained samples were denoted as ZSM-5 (0), ZSM-5 (0.0005), ZSM-5 (0.01), ZSM-5 (0.02), ZSM-5 (0.2) and ZSM-5 (1.0), respectively.

The HCl washed sample was obtained by treating 15 g ZSM-5 (1.0) catalyst with 150 ml 0.1 M HCl solution. The mixture was heated to 80 °C and stirred for 1 h. Then the slurry was cooled to room temperature. The zeolites were filtrated and washed to neutral by deionized water. Then the product was dried and calcinated as the above mentioned conditions. The obtained sample was denoted as ZSM-5 (H).

Ni (4.0 wt%) and Mo (12.0 wt%) were loaded on the hierarchical ZSM-5 by incipient wetness impregnation with an aqueous solution containing $(NH_4)_6Mo_7O_{24}{\cdot}4H_2O$ and $Ni(NO_3)_2{\cdot}6H_2O$. After impregnation, the samples were kept overnight at room temperature and dried at 120 °C for 12 h. At last the samples were calcinated at 450 °C (heating rate 5 °C/min) for 4.5 h.

2.3. Catalyst characterizations

X-ray diffraction (XRD) was used to determine the structural properties of the hierarchical ZSM-5 samples on D/MAX-2500 X-ray diffractometer with (Cu Kα) radiation at 40 kV and 140 mA. Samples were measured in the 2θ range from 5° to 90°. Elemental analysis of Ni and Mo loading was determined by X-Ray Fluorescence (XRF, S4 Pioneer, Bruker). Porous properties of catalysts were determined by N_2 adsorption and desorption isotherms (N_2-BET, Micromeritics Tristar, Micromeritics). Before the measurements, the samples were degassed under vacuum at 300 °C for 4 h. In order to avoid the effects of tensile strengthen, adsorbate phase transitions, and monolayer formation in hierarchical materials [33], the mesopore size distributions were derived using the non-local density functional theory (NLDFT) model. Ammonia temperature programmed desorption (NH_3-TPD) were performed on a Chemisorption Physisorption Analyzer (AMI-300, Altamira Instruments) equipped with a thermal conductivity detector (TCD). For the NH_3-TPD analysis, the samples were pretreated at 450 °C in He for 1 h. After the samples cooled to 100 °C, NH_3 adsorption was performed by the mixture of NH_3 and He (20% NH_3 in He) and then keeping at 100 °C for 10 min. Subsequently a flow of He was passed through the reactor for 120 min to remove weakly adsorbed NH_3 from the zeolite. TPD of NH_3 was monitored in the range of 100–600 °C. The relative concentrations of Lewis and Brønsted acid sites were determined by infrared spectroscopy of adsorbed pyridine (Py-IR, VERTEX 70, Bruker) at 150 and 300 °C. The self-support zeolite wafers (20 mg) were heated to 400 °C at 10 °C/min in air and held for 1 h at 400 °C, and cooled to 300 and 150 °C at 10 °C/min to record the background prior to adsorption experiments. Pyridine was injected into the cell. Then the cell was left in flowing N_2 for 30 min to allow the physisorbed pyridine to be desorbed. Spectra were recorded and averaged over 64 scans between 1300 and 4000 cm^{-1}. The quantitative analysis of Brønsted and Lewis acid sites was carried out using the absorption at 1545 and 1450 cm^{-1}, respectively [34]. The absolute amount of pyridine adsorbed on Brönsted acid sites and Lewis acid sites can be calculated by the following equations:

$$C(B) = \frac{1.67 \times IA(B) \times R^2}{m} \quad (1)$$

$$C(L) = \frac{2.22 \times IA(L) \times R^2}{m} \quad (2)$$

where C is the concentration (μmol/g catalyst), $IA(B,L)$ is the integrated absorbance of Brønsted or Lewis band (cm^{-1}), R is the radius of catalyst disk (cm) and m is the weight of samples (g).

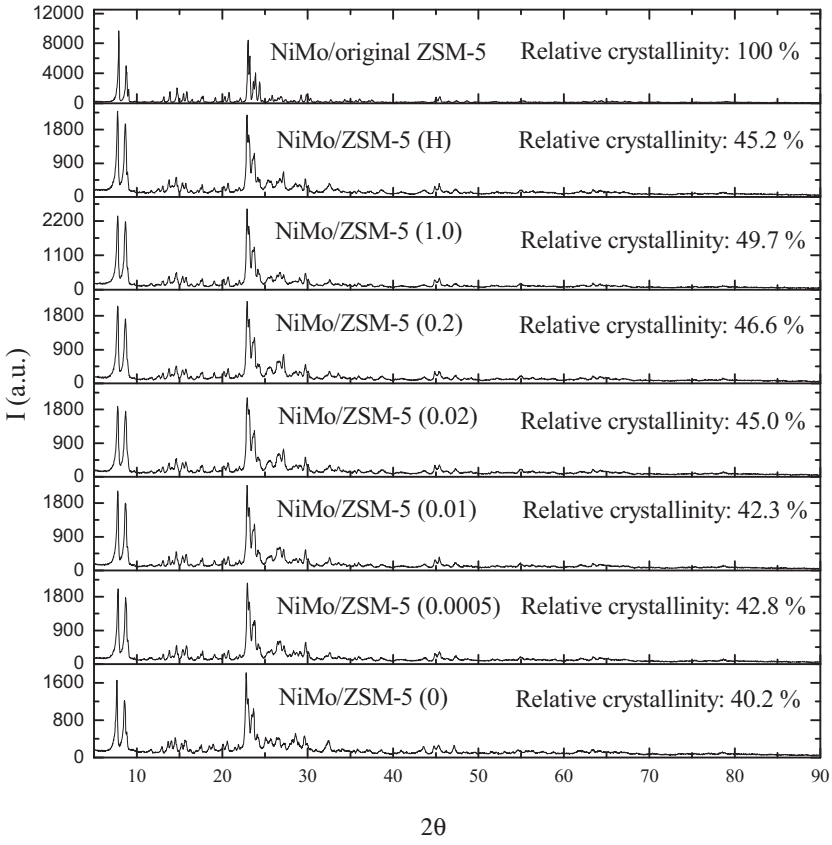

Fig. 1. XRD patterns of the series NiMo/ZSM-5 catalysts.

2.4. Catalytic hydroconversion of soybean oil

The hydroconversion of soybean oil was conducted in a fixed-bed flow reactor (1.2 cm i.d. and 45 cm in length). The reaction temperature was controlled by three thermocouples on the reactor wall and monitored with a thermocouple in the catalyst bed. 10 g of catalyst was loaded and fixed by SiC to get sufficient catalyst-bed length in the reactor. The solution of 25 wt% soybean oil in cyclohexane was used as feedstock and supplied at a flow of 0.8 mL/min with a high-pressure pump. The reaction conditions were carried out at 380 °C under 3 MPa with H_2 flow of 400 mL/min. All catalysts were presulfided in situ at 320 °C and 3.0 MPa for 4 h using 3.0 wt% CS_2 in cyclohexane.

The products were collected after the reaction reached stable, and the products were separated into gas and liquid fractions in a separator. The gaseous products were analyzed online with an Agilent 3000 gas chromatograph equipped with a TCD using three columns (molecular sieve, plot U and alumina). The liquid fraction was divided in two parts: water and organic liquid products (OLPs). The weight of water was measured. The OLPs were qualitatively analyzed with an Agilent 6890N gas chromatography/5975N mass spectrometry (GC/MS). A gas chromatographs (Bruker 456 GC, Bruker), equipped with a flame ionization detector (FID) and a commercially column (ZB-5 HT, 60 m × 0.25 mm × 0.25 μm), was used to quantitatively analyze the hydrocarbons in OLPs. Tetracosane was used as internal standard to quantify the different hydrocarbons produced.

The effects of solvent on the product distribution were identified by a preliminary experiment, which was carried out under the given conditions only using the solvent cyclohexane (the blank experiment). Then the conversion and selectivity were calculated according to following equations:

$$\text{Conversion} = \frac{(G_{\text{feed}} - G_{\text{product}})}{G_{\text{feed}}} \quad (3)$$

$$\text{Selectivity}_{(\text{CH})_n} = \frac{(\text{CH})_{n\,\text{product}}}{\sum(\text{CH})_{n\,\text{product}}} \quad (4)$$

where G_{feed} and G_{product} are the weights of soybean oil in the feed and in the products, respectively, $(\text{CH})_{n\ \text{product}}$ is the weight of C_n hydrocarbon in the products.

3. Results and discussion

3.1. Characterization of the catalysts

All the samples had the same characteristic peaks of XRD pattern in the range of 6–9° and 22.5–25.0° (see Fig. 1). This indicated that the MFI structure in ZSM-5 was maintained after NaOH and HCl treatment [28]. The relative crystallinity was calculated based on the sum of peak intensities for 6–9° and 22.5–25.0°. The relative crystallinity of the NaOH treated and HCl washed samples decreased to 40.2–50% of the original ZSM-5 zeolite. The result of XRF showed that the Ni and Mo loadings were about 4.0 and 12.0 wt%, respectively. The N_2 adsorption–desorption isotherms and the corresponding mesopore size distribution using NLDFT model are illustrated in Fig. 2. Type IV isotherms with remarkable hysteresis loops appeared at higher relative pressures indicated the presence of both micro and mesopores [35]. The parallel disposition of the adsorption and desorption branches suggested the open

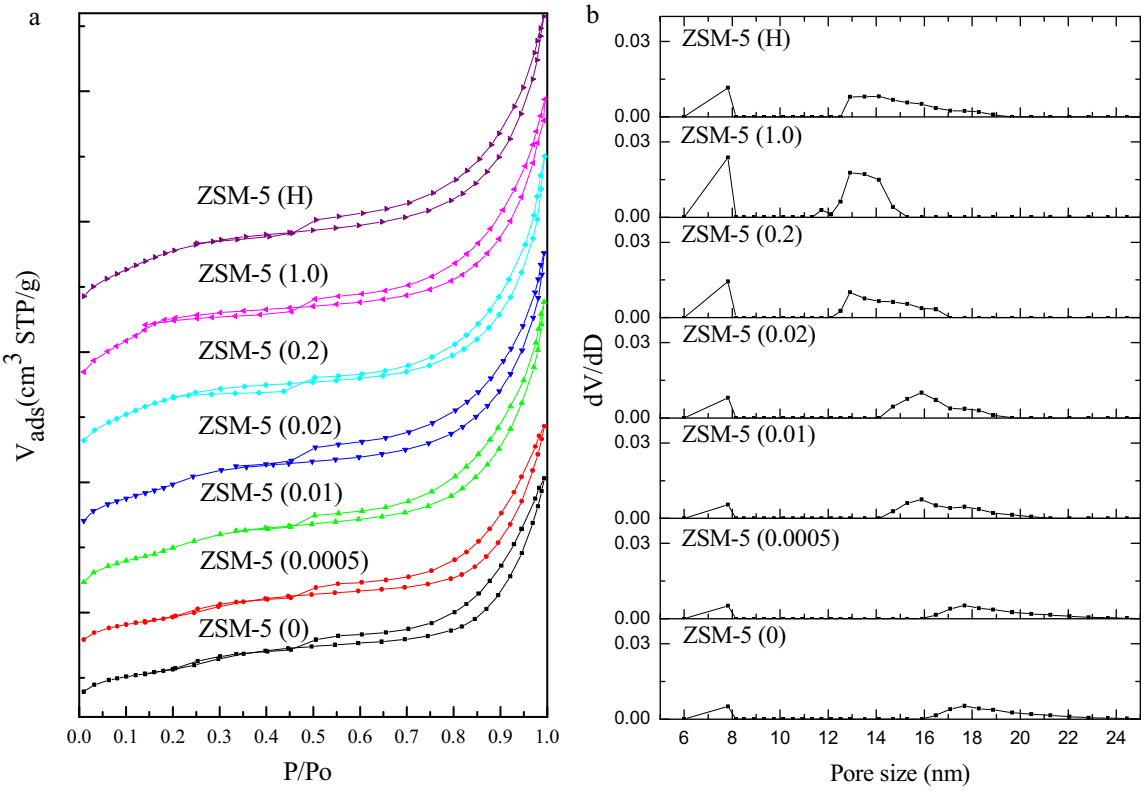

Fig. 2. (a) N_2-adsorption and desorption isotherms of series ZSM-5 zeolites exchanged by various NH_4NO_3 concentration and (b) the mesopore size distribution of series ZSM-5 zeolites using NLDFT model.

mesopores connected to the outer surface [36]. For all the hierarchical samples, the mesopores distribution were both centered at around 7–8 and 14–18 nm. As the degree of NH_4^+ exchange increased, the pore size of larger mesopores shifted from 18 to 13 nm and no change was found for the mesopores around 8 nm. The textural properties of the series ZSM-5 and NiMo/ZSM-5 catalysts are shown in Table 2. For all the NaOH treated ZSM-5 samples, the S_{BET} were all about 300–310 m^2/g. But after the incorporation of metals, the surface areas decreased significantly, about to 230–250 m^2/g. With the NH_4^+ ion exchange, total surface areas S_{BET} and mesopore surface areas S_{meso} increased a little. After mild HCl washing, the surface area increased obviously.

The acidity properties were further investigated by Py-IR and NH_3-TPD. As shown in Fig. 3, two NH_3 desorption peaks were observed at 216–230 and 400–460 °C which were usually assigned to the weak and strong acid sites [37,38]. The acid distribution is listed in Table 3. The acidity mainly came from the weak acid sites when the NH_4NO_3 concentration was lower than 0.02 M. The weak and strong acidity in catalysts were recovered after exchanged. The acidity distribution and the strength of the acid sites depended on the concentration of NH_4NO_3. The temperature peak of the weak acid sites shifted to lower and to the reverse for the strong acid sites with the increase of exchanged NH_4^+ amount. It was concluded that the strength of weak acid sites decreased but increased for the strong acid sites as the degree of NH_4^+ exchange increased. From the result of pyridine adsorption, it was found that the Brønsted acidity was recovered and a little change was observed for Lewis acidity with respect to NH_4^+ ion exchange (see Table 3).

Table 2
Textural properties of series ZSM-5 and NiMo/ZSM-5 catalysts.

	S_{BET}[a] (m^2/g)	$S_{ext/mes}$[a] (m^2/g)	S_{micro}[a] (m^2/g)	V_{meso}[b] (cm^3/g)	V_{micro}[b] (cm^3/g)
ZSM-5 (0)	303.7	126.1	177.6	0.163	0.088
	(247.1)[c]	(110.3)[c]	(136.8)[c]	(0.147)[c]	(0.064)[c]
ZSM-5 (0.0005)	308.8	127.1	181.6	0.168	0.095
	(254.3)[c]	(120.4)[c]	(133.9)[c]	(0.144)[c]	(0.062)[c]
ZSM-5 (0.01)	308.5	136.1	172.4	0.188	0.081
	(251.9)[c]	(127.4)[c]	(124.5)[c]	(0.159)[c]	(0.058)[c]
ZSM-5 (0.02)	313.5	137.5	176.0	0.180	0.082
	(248.7)[c]	(136.3)[c]	(112.4)[c]	(0.164)[c]	(0.051)[c]
ZSM-5 (0.2)	310.4	136.7	173.7	0.180	0.098
	(247.9)[c]	(128.4)[c]	(119.5)[c]	(0.167)[c]	(0.067)[c]
ZSM-5 (1.0)	314.1	136.2	177.9	0.188	0.100
	(244.6)[c]	(135.9)[c]	(108.7)[c]	(0.163)[c]	(0.051)[c]
ZSM-5 (H)	356.0	152.7	203.3	0.183	0.093
	(247.6)[c]	(136.1)[c]	(111.5)[c]	(0.152)[c]	(0.053)[c]

[a] Specific surface area.
[b] Pore volume.
[c] The number of the support supported NiMo.

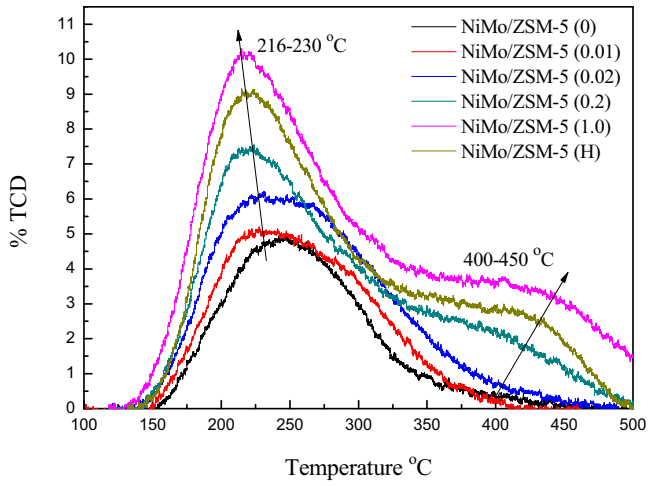

Fig. 3. NH_3-TPD results of series NiMo/ZSM-5 catalysts.

The increase of Brønsted acidity for the hierarchical ZSM-5 samples could be attributed to the formation of new Brønsted acid sites by replacing Na^+ with NH_4^+ after calcinated [39]. For NiMo/ZSM-5 (H) catalyst, 12.6% of weak acidity and 8.4% of strong acidity were removed determined by NH_3-TPD compared with NiMo/ZSM-5 (1.0) catalyst after HCl washed (see Table 3). This may be because that the HCl washing removed the Al species locating at the external surface of the mesopores [40].

3.2. Catalytic conversion of soybean oil

The hydroconversion of soybean oil over the hierarchical catalysts were investigated. The products distribution over NiMo/ZSM-5 (0), NiMo/ZSM-5 (0.0005) and NiMo/ZSM-5 (0.01) are shown in Fig. 4. For these catalysts, no deactivation was observed. As shown in Fig. 4a, the OLPs obtained were mainly paraffins and only a small amount of aromatics was observed over the NiMo/ZSM-5 (0.01) catalyst. The products over NiMo/ZSM-5 (0) were mainly composed of the diesel-range (C_{16}–C_{18}) hydrocarbons with the total selectivity above 76.2%. Moreover, the selectivity of C_{17} and C_{15} hydrocarbons was higher than C_{18} and C_{16} hydrocarbons over NiMo/ZSM-5 (0) catalyst, which meant that the deoxygenation pathway of soybean oil was mainly through decarboxylation and/or decarbonylation (DCOx) rather than hydrodeoxygenation (HDO) reaction [41]. While the major products changed into the C_4–C_8 hydrocarbons for NiMo/ZSM-5 (0.0005) and NiMo/ZSM-5 (0.01) catalysts (see Fig. 4a). 89.5% and 92.1% selectivity for C_4–C_8 were detected, respectively, due to the large degree of cracking.

The further increased NH_4^+ modification had a huge impact on the catalytic performance on the products distribution. It is remarkable that after this treatment, the aromatic compounds were

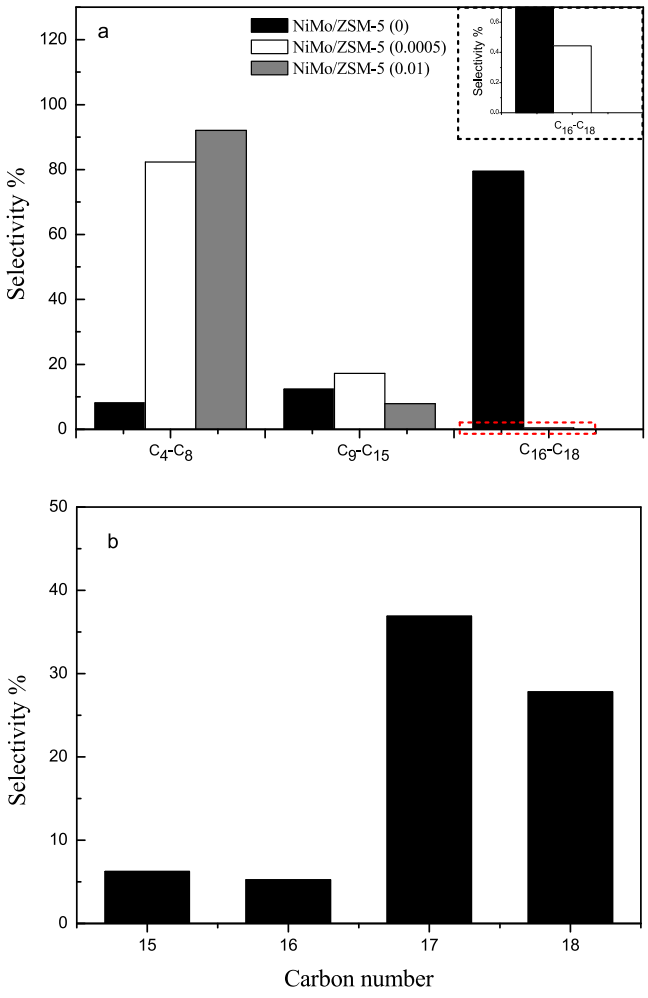

Fig. 4. (a) Selectivity of different product fractions obtained over NiMo/ZSM-5 (0), NiMo/ZSM-5 (0.0005) and NiMo/ZSM-5 (0.01) and (b) selectivity of C_{15}–C_{17} hydrocarbons over NiMo/ZSM-5 (0) catalyst.

formed and became the major products over the catalysts with higher NH_4^+ exchange degree (see Fig. 5). As shown in Fig. 5a, aromatics began to be detected over NiMo/ZSM-5 (0.01) and then the selectivity of aromatics increased sharply. As the NH_4^+ concentration increased to 1.0 M (NiMo/ZSM-5 (1.0)), the selectivity of aromatics reached up to 64.7%. But after further acid treatment, the aromatics selectivity decreased to 54.6%. The result showed that the formation of aromatic compounds strongly depended on the acid sites distribution, especially the Brønsted acid sites of the support. For the NiMo/ZSM-5 (0.01) catalyst, only toluene, ethyl benzene and xylene were detected and *p*-xylene was the most prominent product. This was consistent with the results using HZSM-5 and silica-alumina to convert biofuel into hydrocarbons [42]. When the

Table 3
Acidity properties of series NiMo/ZSM-5 catalysts.

Catalyst	Weak (mmol/g)			Strong (mmol/g)			Total
	L (py)	B (py)	B/L	L (py)	B (py)	B/L	B/L
NiMo/ZSM-5 (0)	0.1428	0.0121	0.08	0.0727	0.0077	0.11	0.09
NiMo/ZSM-5 (0.0005)	0.1447	0.0169	0.12	0.0689	0.0329	0.48	0.23
NiMo/ZSM-5 (0.01)	0.1465	0.0224	0.15	0.0684	0.0402	0.59	0.29
NiMo/ZSM-5 (0.02)	0.1495	0.0250	0.17	0.0671	0.0453	0.67	0.32
NiMo/ZSM-5 (0.2)	0.1504	0.0285	0.19	0.0724	0.0526	0.73	0.36
NiMo/ZSM-5 (1.0)	0.1554	0.0318	0.20	0.0751	0.0579	0.77	0.39
NiMo/ZSM-5 (H)	0.1359	0.0278	0.20	0.0669	0.0549	0.82	0.41

L (py) and B (py), Lewis and Brønsted acidity determined by Py-IR.

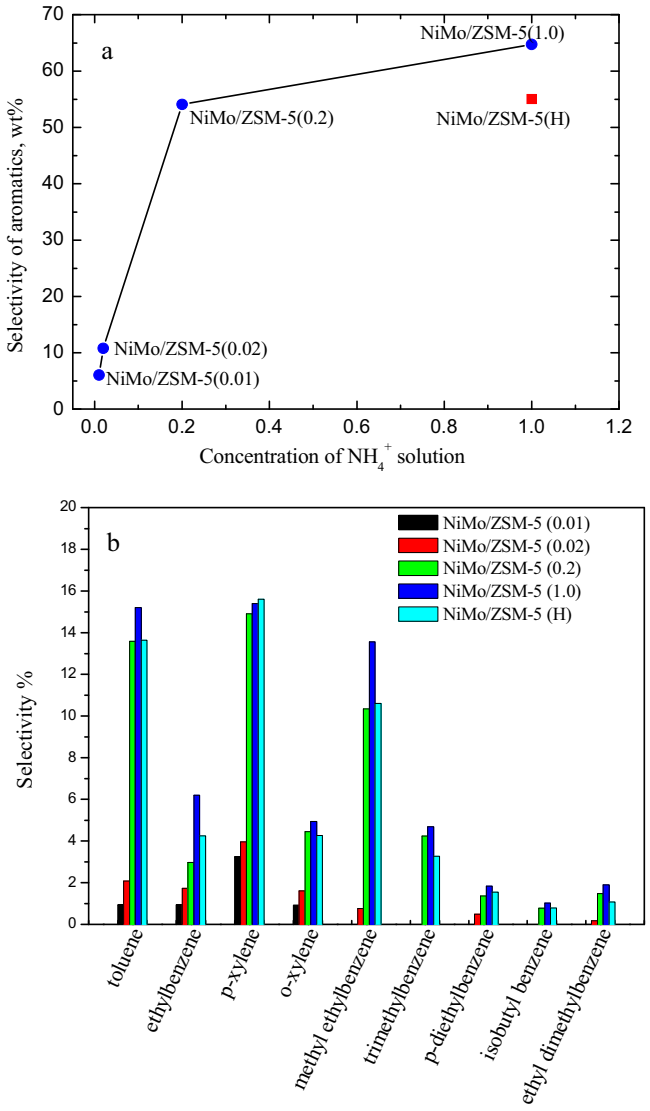

Fig. 5. Selectivity of (a) total aromatic compounds obtained and (b) different aromatic compounds obtained over series ZSM-5 catalysts.

NH_4^+ concentration increased to 0.02 M (NiMo/ZSM-5 (0.02)), the selectivity of toluene, ethyl benzene and xylene increased and other three new aromatics methyl ethyl benzene, *p*-diethylbenzene and ethyl dimethylbenzene were first to be detected. For NiMo/ZSM-5 (0.2) catalyst, the selectivity for all the above-mentioned aromatics increased sharply and trimethylbenzene and isobutyl benzene began to be detected. The aromatic distribution is shown in Fig. 5b. So it could be concluded that the formation of the heavy aromatics (methyl ethyl benzene, *p*-diethyl benzene, trimethylbenzene, isobutyl benzene and ethyl dimethyl benzene) was harder than the lighter aromatics (toluene, ethyl benzene and xylene). Toluene, methyl ethyl benzene and xylene, especially the *p*-xylene, were the primary products for the samples with high NH_4^+ exchange degree.

Here, we proposed a whole reaction scheme for quantitative conversion of triglycerides to desirable products over hierarchical ZSM-5 catalyst as shown in Schemes 1 and 2. As reported, the triglycerides were first diffused and adsorbed on the surface of the metal active sites (Ni-Mo-S) to produce hydrocarbons via DCOx and HDO as shown in Scheme 1 [5,43]. After deoxygenation, the hydrocarbons produced were cracked to form the C_4–C_8 hydrocarbons, olefins and then the aromatics. Bakhshi and coworkers [44] found that the aromatics were produced by aromatization reactions of C_2-C_{10} olefins in the pore of catalyst during catalytic conversion of canola oil over potassium-impregnated ZSM-5, and the acidity of Brønsted and total acid sites severely affected the aromatization reaction. Rodewald *et al.* [45] discovered that the olefins were first transformed to naphthenes and then aromatics were formed by hydrogen transfer from naphthenes. Recently, it was further proposed that the aromatics were formed by Diels–Alder reactions of olefins [46]. Therefore, a reaction route for the conversion of triglycerides to hydrocarbons and aromatics catalyzed by the hierarchical ZSM-5 was proposed. The cracking and dehydrogenation of paraffins occurred on the Brønsted acid sites to form the olefins. Then the formed olefins came to the Lewis acid site to undergo Diels–Alder cyclization reactions to produce the cycloalkanes. At last the cycloalkanes transformed into the aromatics at Brønsted acid sites by dehydrogenation-aromatization.

The physical properties of the supports, active phase and compositions were almost the same for all catalysts. So it was inferred that the differences of products distribution were due to the acidity of the support. For NiMo/ZSM-5 (0) catalyst, there was relatively low Brønsted acidity and strong acidity. Thus it produced a small amount of cracking products. For NiMo/ZSM-5 (0.0005) and NiMo/ZSM-5 (0.01) catalysts, the ion exchange by NH_4^+ recovered partly the strong acidity and Brønsted acidity. So the selectivity to C_4–C_8 increased sharply to 89.5% and 92.1%, respectively. As Brønsted acidity further increased, aromatics were formed and the selectivity of aromatics reached up to 64.7% for NiMo/ZSM-5 (1.0) sample. The strong acid sites and Brønsted acid sites favored the cracking reaction as reported [47,48]. So the strong acidity and Brønsted acidity modified by NH_4NO_3 had the most significant effect on the cracking and the formation of aromatic compounds.

The variation of the olefins, a significant factor in designing a feasible process for aromatics production, in gas products for different catalysts was investigated. With increasing concentration of Brønsted acid sites, the difference in yields of cracking and dehydrogenation increased. As shown in Fig. 6, the total yield of organic gas increased as the Brønsted acidity density increased from NiMo/ZSM-5 (0.0005) to NiMo/ZSM-5 (1.0) samples. For NiMo/ZSM-5 (0.0005) catalyst, no ethylene was obtained and the yields of propylene and butene were 0.06% and 0.15%, respectively. A large amount of propylene and butene were formed when the NH_4^+ concentration was higher than 0.01 M. Ethylene was not detected until the Brønsted acidity density was 0.0811 mmol/g (for NiMo/ZSM-5 (0.2) sample). This was mainly due to the direct cracking and dehydrogenation of alkanes on strong acid sites and Brønsted acid sites. However, the result of NiMo/ZSM-5 (H) catalyst was out of expected. Compared with NiMo/ZSM-5 (0.2) catalyst, the Lewis acidity of NiMo/ZSM-5 (H) sample was lower but Brønsted acidity was the same. However, the yield of olefins over this catalyst was higher than that of NiMo/ZSM-5 (0.2). This may be because of the decrease of Lewis acidity led to the low degree of Diels–Alder cyclization reactions as discussed below. In addition, many works showed that the catalytic dehydrogenation of alkanes like propane and butane to form the gaseous olefins might occur on the Brønsted acid sites [49–51]. These results indicated that the formation of olefins strong depends on the Brønsted acid density.

According to the literatures, the Diels–Alder cyclization reactions relied on Lewis acidity of the catalysts to a great extent [52–57]. Lewis acid site were able to activate enone dienophiles by lowering the activation barrier in the Diels–Alder reactions of enones [55]. So the Brønsted and Lewis acidity influenced the formation of aromatics. After the NH_4^+ exchange, the Brønsted acidity was tuned while the Lewis acidity only changed little. From NiMo/ZSM-5 (0.0005) to NiMo/ZSM-5 (0.01) catalysts, the increased Brønsted acidity promoted the cracking reaction but the amount of Brønsted acid sites was not enough to produce aromatics. When the Brønsted/Lewis (B/L) reached 0.29 for NiMo/ZSM-5

$$RCH_2COOH + 3H_2 \longrightarrow RCH_2CH_3 + 2H_2O$$

$$RCH_2COOH + H_2 \longrightarrow RCH_3 + H_2O + CO$$

$$RCH_2COOH \longrightarrow RCH_3 + CO_2$$

Scheme 1. Proposed pathways for the deoxygenation of fatty acids.

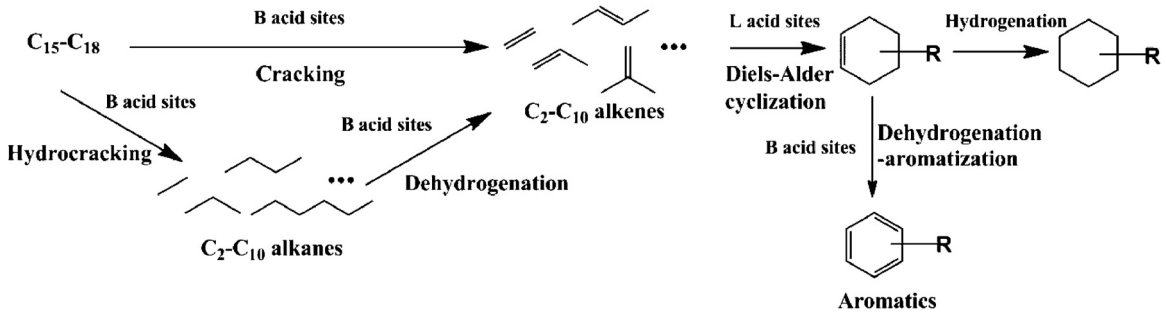

Scheme 2. Proposed pathways for the formation of aromatics.

(0.01), aromatization reactions began to occur and aromatics was detected. With the B/L up to 0.36 for NiMo/ZSM-5 (0.2) catalyst, large amount of aromatics were produced due to the high Brønsted acid density. The further increased B/L (0.39) for NiMo/ZSM-5 (1.0) catalyst gave a higher yield of aromatics. However, for NiMo/ZSM-5 (H) sample, the yield of gaseous olefins decreased due to the reduction of Lewis and Brønsted acidity (see Fig. 6) and so did the selectivity of total aromatics. Moreover, methyl cyclohexane and toluene were chosen as the target product to further certify the role of Lewis and Brønsted acidity in the Diels–Alder and dehydrogenation–aromatization. The distribution of methyl cyclohexane and toluene over NiMo/ZSM-5 (0.2), NiMo/ZSM-5 (1.0) and NiMo/ZSM-5 (H) is shown in Fig. 7. For NiMo/ZSM-5 (0.2) and NiMo/ZSM-5 (1.0) catalysts, the total selectivity of methyl cyclohexane and toluene was almost the same due to the almost same Lewis acidity which favored the Diels–Alder cyclization reaction. The NiMo/ZSM-5 (1.0) catalyst with more Brønsted acidity gave a higher selectivity to toluene by expense of methyl cyclohexane by dehydrogenation–aromatization. For NiMo/ZSM-5 (H) catalyst, the Lewis acidity was lower than NiMo/ZSM-5 (0.2) and NiMo/ZSM-5 (1.0) catalysts but the Brønsted acidity was the same with NiMo/ZSM-5 (0.2). Therefore, the total selectivity of methyl cyclohexane and toluene was lower, but with a similar selectivity of toluene with NiMo/ZSM-5 (0.2) catalyst.

As shown in Fig. 5, the ability to form various aromatic compounds was different. Heavy aromatics were harder than the lighter aromatics. R. Choudhary [58] found that the stronger acid sites favored the dealkylation of the higher aromatics. The decrease in

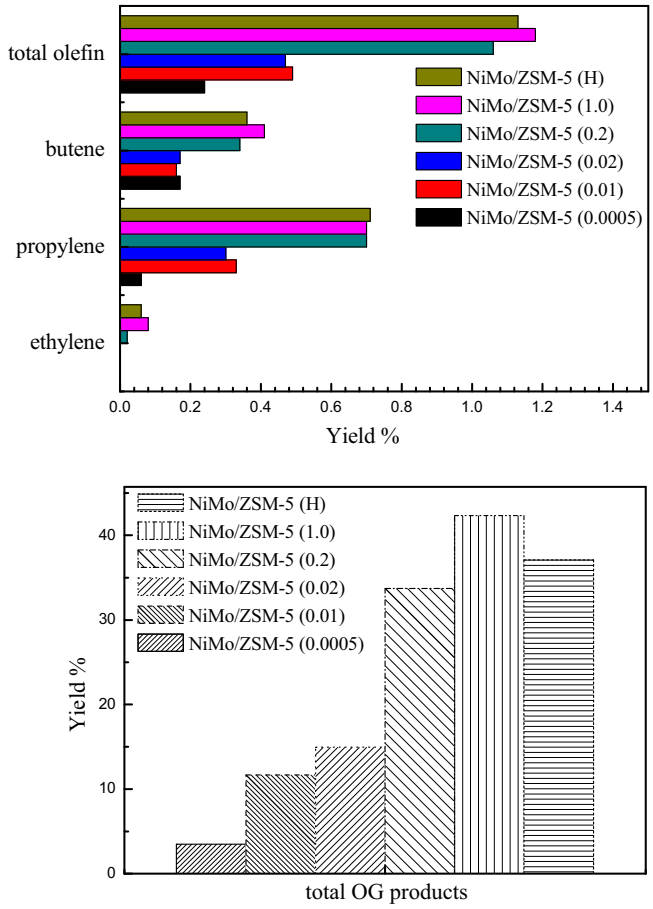

Fig. 6. Distributions of olefins products in deoxygenation of soybean oil over series NiMo/ZSM-5 catalysts (OG, organic gas).

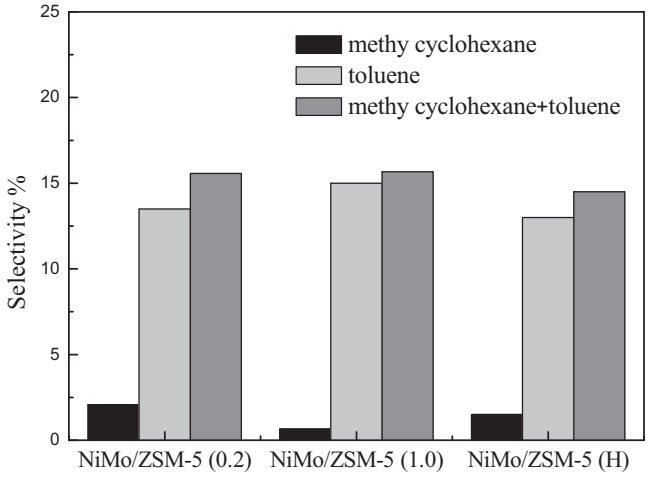

Fig. 7. Selectivity of methyl cyclohexane and toluene obtained over NiMo/ZSM-5 (0.2), NiMo/ZSM-5 (1.0) and NiMo/ZSM-5 (H).

the selectivity for higher aromatics was because of the lower reactivity of these aromatics and the increased strength of stronger acid sites. The result of NH_3-TPD showed that the strength of the strong acid sites became stronger as the concentration of NH_4^+ increased. As for the NiMo/ZSM-5 (0.01) and NiMo/ZSM-5 (0.02) with low NH_4^+ concentration, the strength of strong acid sites was not high enough to produce the higher aromatics because of their low reactivity. Therefore, only toluene, ethyl benzene and xylene were formed. As the increase of NH_4^+ concentration, the heavy aromatics appeared and the amount increased with the acid strength. The *p*-xylene dominated the organic liquid products could be assigned to the shape selectivity of hierarchical ZSM-5 and the isomerization of *m*-xylene [40,59].

4. Conclusions

The quantitative conversion of triglycerides to desirable production with high selectivity was obtained over hierarchical ZSM-5 catalysts. A series of catalysts with different acid properties were obtained by tuning NH_4^+ exchange. The C_{16}–C_{18} hydrocarbons were mainly obtained over the catalyst without NH_4^+ exchange due to the low Brønsted and strong acidity. But the major products changed into the gasoil-range hydrocarbons for the samples with low NH_4^+ exchange amount (NiMo/ZSM-5 (0.0005) and NiMo/ZSM-5 (0.01)). This was because of the recovery of Brønsted acidity by NH_4^+ exchange. As the NH_4^+ concentration further increased higher than 0.2 M, the amount of aromatic compounds increased significantly and became the dominant products. The formation of aromatics was attributed to the Diels–Alder cyclization and dehydrogenation–aromatization of olefins on Lewis and Brønsted acid sites. The olefins were obtained by cracking or dehydrogenation. Lewis acid sites favored the Diels–Alder cyclization of the olefins to form the cycloalkanes. Nevertheless, the dehydrogenation–aromatization reaction to form the aromatics was restricted by Brønsted acid sites. The formation of heavy aromatics was much more difficult than the lighter aromatics, which were dependent on the strength of strong acid sites and the reactivity of these aromatics. The work presented here provided a guideline for designing a catalyst with excellent catalytic performance for the desirable products.

Acknowledgements

The financial supports by National Natural Science Foundation of China (Grant No. 21476169, 21476168) are gratefully acknowledged. The authors thank Ms. Yuhan Yang, Mr. Lun Pan and Yawei Shi for their help with catalytic evaluation and Mr. Qiang Deng for his guidance for alkali treatment.

References

[1] M. Stöcker, Angew. Chem. Int. Ed. 47 (2008) 9200–9211.
[2] G.W. Huber, S. Iborra, A. Corma, Chem. Rev. 106 (2006) 4044–4098.
[3] I. Kubičková, D. Kubička, Waste Biomass Valor. 1 (2010) 293–308.
[4] J.N. Chheda, G.W. Huber, J.A. Dumesic, Angew. Chem. Int. Ed. 46 (2007) 7164–7183.
[5] C. Zhao, T. Brück, J.A. Lercher, Green Chem. 15 (2013) 1720–1739.
[6] H. Fukuda, A. Kondo, H. Noda, J. Biosci. Bioeng. 92 (2001) 405–416.
[7] B.L. Salvi, N.L. Panwar, Renew. Sustain. Energy Rev. 16 (2012) 3680–3689.
[8] J. Liu, C. Liu, G. Zhou, S. Shen, L. Rong, Green Chem. 14 (2012) 2499–2505.
[9] G. Knothe, Prog. Energy Combust. Sci. 36 (2010) 364–373.
[10] S.K. Saxena, N. Viswanadham, Fuel Process. Technol. 119 (2014) 158–165.
[11] D. Verma, R. Kumar, B.S. Rana, A.K. Sinha, Energy Environ. Sci. 4 (2011) 1667–1671.
[12] B. Peng, Y. Yao, C. Zhao, J.A. Lercher, Angew. Chem. Int. Ed. 51 (2012) 2072–2075.
[13] S.K. Kim, J.Y. Han, H.-S. Lee, T. Yum, Y. Kim, J. Kim, Appl. Energy 116 (2014) 199–205.
[14] F. Pinto, S. Martins, M. Gonçalves, P. Costa, I. Gulyurtlu, A. Alves, B. Mendes, Appl. Energy 102 (2013) 272–282.
[15] G.W. Huber, A. Corma, Angew. Chem. Int. Ed. 46 (2007) 7184–7201.
[16] J. Cheng, T. Li, R. Huang, J. Zhou, K. Cen, Bioresour. Technol. 158 (2014) 378–382.
[17] S.P.R. Katikaneni, J.D. Adjaye, N.N. Bakhshi, Energy Fuel 9 (1995) 599–609.
[18] F.A.A. Twaiq, A.R. Mohamad, S. Bhatia, Fuel Process. Technol. 85 (2004) 1283–1300.
[19] Y.-C. Yao, J.-H. Tsai, Aerosol Air Qual. Res. 13 (2013) 739–747.
[20] S.A. Khabbaz, R. Mobasheri, Fuel 123 (2014) 26–32.
[21] C.L. Williams, C.-C. Chang, P. Do, N. Nikbin, S. Caratzoulas, D.G. Vlachos, R.F. Lobo, W. Fan, P.J. Dauenhauer, ACS Catal. 2 (2012) 935–939.
[22] E. Santillan-Jimenez, M. Crocker, J. Chem. Technol. Biotech. 87 (2012) 1041–1050.
[23] D. Kubička, J. Horáček, M. Setnička, R. Bulánek, A. Zukal, I. Kubičková, Appl. Catal. B-Environ. 145 (2014) 101–107.
[24] C. Wang, Z. Tian, L. Wang, R. Xu, Q. Liu, W. Qu, H. Ma, B. Wang, ChemSusChem 5 (2012) 1974–1983.
[25] N. Chen, S. Gong, H. Shirai, T. Watanabe, E.W. Qian, Appl. Catal. A Gen. 466 (2013) 105–115.
[26] W. Song, C. Zhao, J.A. Lercher, Chem. Eur. J. 19 (2013) 9833–9842.
[27] I.I. Ivanova, E.E. Knyazeva, Chem. Soc. Rev. 42 (2013) 3671–3688.
[28] S. Sartipi, K. Parashar, M.J. Valero-Romero, V.P. Santos, B. van der Linden, M. Makkee, F. Kapteijn, J. Gascon, J. Catal. 305 (2013) 179–190.
[29] D.P. Serrano, R.A. García, G. Vicente, M. Linares, D.J. Procházková, J. Čejka, J. Catal. 279 (2011) 366–380.
[30] X. Zhu, L.L. Lobban, R.G. Mallinson, D.E. Resasco, J. Catal. 271 (2010) 88–98.
[31] J.A. Botas, D.P. Serrano, A. García, R. Ramos, Appl. Catal. B-Environ. 145 (2014) 205–215.
[32] J. Kang, K. Cheng, L. Zhang, Q. Zhang, J. Ding, W. Hua, Y. Lou, Q. Zhai, Y. Wang, Angew. Chem. Int. Ed. 50 (2011) 5306–5309.
[33] J.C. Groen, L.A.A. Peffer, J. Pérez-Ramıírez, Micropor. Mesopor. Mater. 60 (2003) 1–17.
[34] E.P. Parry, J. Catal. 2 (1963) 371–379.
[35] J.C. Groen, L.A.A. Peffer, J.A. Moulijn, J. Pérez-Ramıírez, Colloids Surf. A: Physicochem. Eng. Aspects 241 (2004) 53–58.
[36] J.C. Groen, L.A. Peffer, J.A. Moulijn, J. Pérez-Ramıírez, Chem. Eur. J. 11 (2005) 4983–4994.
[37] X. Li, S. Liu, X. Zhu, Y. Wang, S. Xie, W. Xin, L. Zhang, L. Xu, Catal. Lett. 141 (2011) 1498–1505.
[38] S.-H. Kang, J.-H. Ryu, J.-H. Kim, P.S.S. Prasad, J.W. Bae, J.-Y. Cheon, K.-W. Jun, Catal. Lett. 141 (2011) 1464–1471.
[39] G.L. Woolery, G.H. Kuehl, H.C. Timken, A.W. Chester, J.C. Vartuli, Zeolites 19 (1997) 288–296.
[40] C. Fernandez, I. Stan, J.P. Gilson, K. Thomas, A. Vicente, A. Bonilla, J. Pérez-Ramıírez, Chem. Eur. J. 16 (2010) 6224–6233.
[41] Y. Yang, Q. Wang, X. Zhang, L. Wang, G. Li, Fuel Process. Technol. 116 (2013) 165–174.
[42] K. Suzuki, T. Noda, N. Katada, M. Niwa, J. Catal. 250 (2007) 151–160.
[43] G.W. Huber, P. O'Connor, A. Corma, Appl. Catal. A Gen. 329 (2007) 120–129.
[44] S.P.R. Katikaneni, J.D. Adjaye, R.O. Idem, N.N. Bakhshi, Ind. Eng. Chem. Res. 35 (1996) 3332–3346.
[45] V.S. Nayak, V.R. Choudhary, Appl. Catal. 9 (1984) 251–261.
[46] A. Corma, G.W. Huber, L. Sauvanaud, P. O'Connor, J. Catal. 247 (2007) 307–327.
[47] W.O. Haag, R.M. Lago, P.G. Rodewald, J. Mol. Catal. 17 (1982) 161–169.
[48] S. Gong, A. Shinozaki, E.W. Qian, Ind. Eng. Chem. Res. 51 (2012) 13953–13960.
[49] R. Gounder, E. Iglesia, J. Catal. 277 (2011) 36–45.
[50] R. Gounder, E. Iglesia, J. Am. Chem. Soc. 131 (2009) 1958–1971.
[51] B. Xu, C. Sievers, S.B. Hong, R. Prins, J.A. van Bokhoven, J. Catal. 244 (2006) 163–168.
[52] V. Eschenbrenner-Lux, P. Küchler, S. Ziegler, K. Kumar, H. Waldmann, Angew. Chem. Int. Ed. 53 (2014) 2134–2137.
[53] E. Jnoff, L. Ghosez, J. Am. Chem. Soc. 121 (1999) 2617–2618.
[54] Y.E. Türkmen, T.J. Montavon, S.A. Kozmin, V.H. Rawal, J. Am. Chem. Soc. 134 (2012) 9062–9065.
[55] H.V. Pham, R.S. Paton, A.G. Ross, S.J. Danishefsky, K.N. Houk, J. Am. Chem. Soc. 136 (2014) 2397–2403.
[56] C.M. Rasik, M.K. Brown, J. Am. Chem. Soc. 135 (2013) 1673–1676.
[57] F. Viton, G. Bernardinelli, E.P. Kündig, J. Am. Chem. Soc. 124 (2002) 4968–4969.
[58] J.D. Adjaye, S.P.R. Katikaneni, N.N. Bakhshi, Fuel Process. Technol. 48 (1996) 115–143.
[59] S. Al-Khattaf, Chem. Eng. Process. 46 (2007) 964–974.